Postprint of: L. Leszkowska, M. Rzymowski, K. Nyka and Ł. Kulas, "Influence of 3D Printed Overlay Infill Patterns on Miniaturized ESPAR Antenna Performance," 2024 25th International Microwave and Radar Conference (MIKON), Wroclaw, Poland, 2024, pp. 173-176, doi: 10.23919/MIKON60251.2024.10633919.

Influence of 3D Printed Overlay Infill Patterns on Miniaturized ESPAR Antenna Performance

Luiza Leszkowska*[1], Mateusz Rzymowski*[2], Krzysztof Nyka*[3], Łukasz Kulas*[4]
*Department of Microwave and Antenna Engineering, Gdansk University of Technology, Faculty of Electronics, Telecommunications and Informatics, Gdansk, Poland
{[1]luiza.leszkowska, [2]mateusz.rzymowski, [3]krzysztof.nyka, [4]lukasz.kulas}@pg.edu.pl

***Abstract*—In this article, we show how different infill patterns influence the overall performance of miniaturized electrically steerable parasitic array radiator (ESPAR) antenna. The use of 3D printed dielectric overlays is a simple and flexible way to miniaturize ESPAR antennas, so they are more compact and can be better integrated with wireless sensor network (WSN) nodes or gateways in different application areas. Additionally, such overlays modify antenna radiation patterns in elevation, which can be used to provide better connectivity with WSN nodes places beneath a WSN gateway. In this work, we investigate 3 different infill patterns that can be used in widely available 3D printers to create the overlay in a 3D printing process, and we show how each of the infill patterns used affects the antenna performance. Finally, based on our measurements, we propose the infill pattern that provides the best parameters of a miniaturized ESPAR antenna.**

Keywords*— *switched-beam antenna, electronically steerable parasitic array radiator (ESPAR), 3D print, energy efficiency, sustainability, wireless sensor network (WSN)

I. Introduction

Wireless sensor network (WSN) nodes or gateways are used for sensing and monitoring in many practical applications, including agriculture, in which they provide up to date information about livestock or crops that can affect production capabilities [1]. Key features important for successful WSN systems deployment involve wireless link reliability, especially in environments like greenhouses, crop fields or buildings with livestock penned indoors, in which propagation conditions may change over time and, in effect, deteriorate link parameters as well as the overall energy efficiency of a deployed WSN solution [2]. To address such requirements, energy efficient reconfigurable antennas that provide electronically steerable directional beams can be used, which can allow for adaptation to varying propagation conditions [3]-[6].

Electrically steerable parasitic array radiator (ESPAR) antennas [6]-[8] are one of the most promising concepts for energy-efficient beam steering. In such antennas, radio frequency (RF) signal source is connecter to a centrally placed monopole, while the antenna radiation pattern is shaped by changing values of load impedances connected to passive monopoles surrounding the centrally placed element. To provide energy efficient ESPAR antennas, that can be successfully integrated within WSN systems, a simplified beam steering concept has been proposed [7],[8]. In this concept single-pole double-throw (SPDT) digitally controlled switches were connected to passive elements' ends to provide switchable load impedances close to an open or short circuit, and, in consequence, to form a directional main beam and to rotate it in the horizontal axis around the ESPAR antenna.

To successfully implement energy-efficient ESPAR antenna within a WSN node having a compact form, one can reduce ESPAR antenna size by embedding the antenna in a homogeneous dielectric material. By using mechanically processed ceramic material having relative permittivity around 4.5 it was possible to reduce the overall antenna footprint by 50% [9]. Such miniaturization can be provided at much lower cost by using 3D printing [10], which also enables easy and fast prototyping. Moreover, using low-cost commonly used polylactic acid (PLA) filaments and varying PLA miniaturization overlays sizes [11] or different filament materials available for 3D printing process [12],[13] one can not only miniaturize the overall antenna size but also modify its vertical radiation patterns, which was overlooked in [9].

To produce an energy efficient miniaturized ESPAR antenna for a WSN node at low cost one has to use 3D printing process to create its dielectric overlay. In the antenna design, dielectric overlay medium used in simulations is homogeneous. However, in the actual production process of such a dielectric element made by low-cost 3D printing it is not possible to provide perfectly homogeneous dielectric structure. In existing publications, it was shown that infill density and shape can deteriorate different antenna designs [14],[15]. Therefore it can also influence the overall performance of energy efficient miniaturized ESPAR antennas.

The aim of this study is to investigate how the use of different infill patterns in productions process of ESPAR antenna dielectric overlays using low-cost 3D printing will influence the resulting miniaturized energy-efficient ESPAR antenna performance.

II. Antenna Design

ESPAR antenna is a type of switched-beam antenna with steering circuit based on SPDT switches, in which switching is performed by changing the state of passive elements between the director and the reflector. The status of each passive element is controlled individually using GPIO pins. Passive elements, likewise the active element, are in the form of monopoles. As part of this study, an antenna with 12 passive elements was designed, which allows for obtaining 12 different directional beams. Switching mechanism placed on the bottom of the printed circuit board (PCB) is based on very low insertion loss (0.23 dB @2.7 GHz) integrated FET switches NJG1681. An additional dielectric overlay has been designed for the antenna, which reduces its size at a low

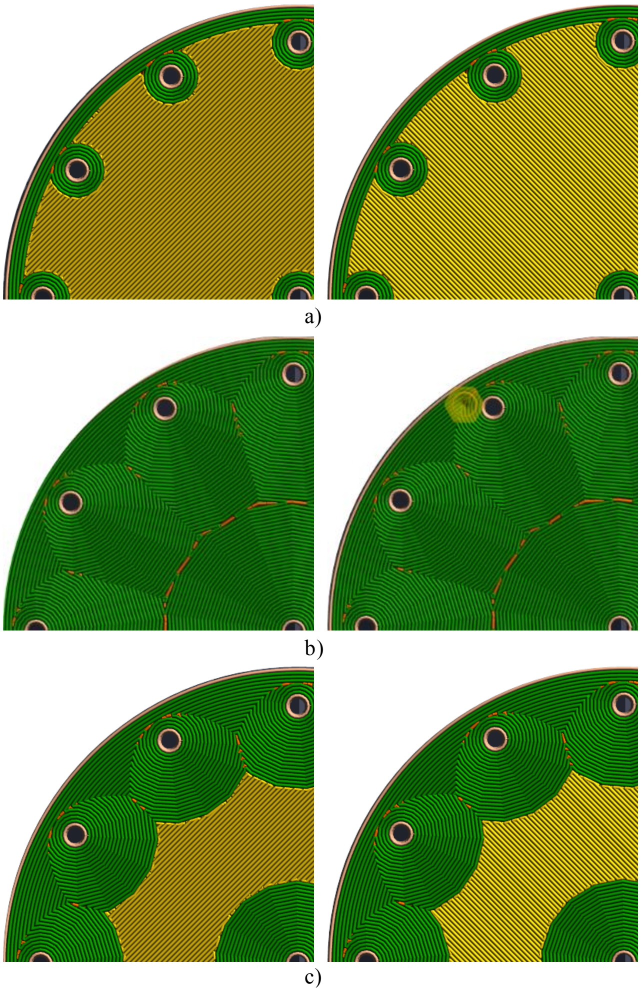

Fig. 1. Two consecutive layers of 3D printed overlay (concentric pattern is marked in green, linear pattern in yellow): a) Infill pattern: linear; b) Infill pattern: concentric; c) Infill pattern: mixed concentric-linear.

cost [11]. The overlay has a cylindrical shape with a diameter of 64.8 mm and a height of 24.4 mm. The antenna overlay was designed using Altair Feko. Within this study, 3 different overlays were produced using 3D printing with 100% infill density but different infill patterns. Each of the infill patterns will be discussed in more detail in the next section. PLA (Polylactic Acid) filament with dielectric constant equal to 2.62 and dielectric loss tangent 0.005 determined by measuring samples printed with the same printer settings, was used to produce all the presented overlays.

III. Antenna Realization and Measurements

A. 3D Printed Overlay Infill Patterns

In the antenna design, the medium used as the dielectric overlay is homogeneous. However, regarding the actual implementation of such a dielectric element made by 3D printing, we are not able to make it perfectly homogeneous. The effective permittivity of a 3D printed dielectric varies for different regions of infill pattern and for different direction of E-field vector. Therefore, it would be virtually impossible to capture precisely the effects of this inhomogeneity and anisotropy on the antenna operation using effective dielectric constant approach. The aim of this study was to produce and compare various overlay infill patterns and verify its influence on miniaturized ESPAR antenna performance. The overlays were printed using a Flashforge Creator 3 printer with a nozzle diameter of 0.4 mm, extrusion temperature of 215°C, bed temperature of 50°C, layer height of 0.2 mm and 100% infill density. Two consecutive layers of 3D printed overlay for each considered infill pattern: linear, concentric and mixed concentric-linear patterns are presented in Fig. 1a), Fig. 1b) and Fig. 1c) respectively.

The first considered infill pattern, presented in Fig. 1Fig. 1 a), is a linear infill, in which the direction of the infill line changes alternately by 90 degrees every layer. Concentric filling occurs only around the active and passive elements as well as on the edge of the overlay. Another infill method taken into account, shown in Fig. 1 b), was the concentric infill pattern, i.e. all lines were printed in circles from the center to the outside of the overlay excluding the area around passive elements. The third option, presented in Fig. 1 c), combines the above solutions by changing the proportions of each filling method, i.e. between the active element and passive elements, the linear filling was kept, but the number of concentric infill outlines around these elements was increased from 5 to 20.

B. Antenna Measurements

The performance of the antenna was verified by measurements in our 11.9 x 5.6 x 6.0 m anechoic chamber. The antenna is produced in such a way that all the overlays are applied to the PCB from above as shown in Fig. 2 and can be freely replaced using a common antenna PCB for all measurements.

Normalized radiation pattern of miniaturized ESPAR antenna printed with three different overlay infill pattern methods in E-plane for two opposing directional beams is shown in Fig. 3. The difference in antenna gain with a concentric infill pattern and a concentric-linear infill pattern is minor and amounts to 0.1 dB. A more significant difference is noticeable considering the reflection coefficient, the antenna version with a concentric infill pattern is better matched, as presented in Fig. 4. The reflection coefficient of antenna with a linear infill pattern is similar to that of an antenna with a concentric infill pattern, however its gain is 0.3 dB lower and concentric infill allows to provide the best matching.

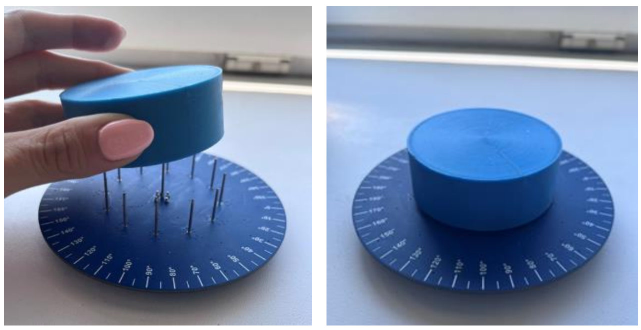

Fig. 2. 3D printed miniaturized ESPAR antenna overlays with a PCB prototype of the ESPAR antenna.

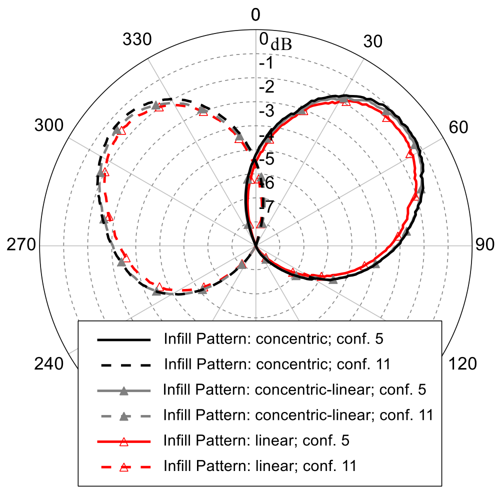

Fig. 3. Normalized radiation patterns of miniaturized ESPAR antenna using 3 different overlay infill pattern methods in E-plane for two opposing directional beams.

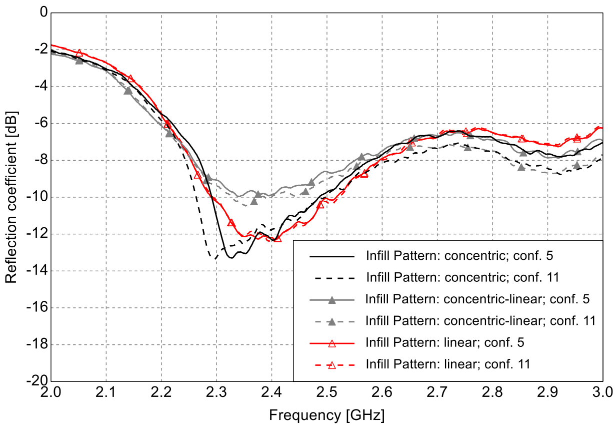

Fig. 4. Reflection coefficient of miniaturized ESPAR antenna printed with 3 different overlay infill pattern methods for two opposing directional beams.

IV. Conclusions

In this article, the influence of different 3D-printed overlay infill patterns on the performance of miniaturized ESPAR antenna was presented. Our considerations were focused on the basic infill variants available in the most common 3D printers as a starting point for further analyses to provide a clear baseline and investigate if such basic infills differences can be observed in measurements. Based on our measurement results, the best infill pattern for 3D printed overlay for miniaturized ESPAR antennas in terms of antenna gain and matching is concentric infill. However, it has to be carefully considered and tested in the antenna design to provide the optimal performance and values of the resulting prototypes. Certainly, there are many possible filling patterns for the considered 3D printed overlays in modern 3D printers, including the possibility of modifying the filling density, which will be investigated in our future works. Systematic repeatability tests are not presented in the this study. They should involve statistical approach and would require a large number of manufactured samples of the overlays, which hasn't been done yet. Instead, we plan to investigate the repeatability measuring the dielectric constant tensor of small samples of printed dielectric having uniform patters. Our next considerations will also include determining the optimal angle of rotation of the lines direction in particular layers for linear infill pattern overlay and modifications of the outline of passive elements and impact of modification of the filling density on the antenna performance for different available materials, including bio-degradable and recyclable ones.

Acknowledgment

This research was funded by the i-MAGS project, which has received funding from the Federal Ministry of Education and Research (BMBF; agreement no. 01DS22002A) and the National Centre for Research and Development (NCBR; agreement no. WPN/4/66/i-MAGS/2022) under 4th Poland – Germany Call for Proposals in the field of Digital Green Technology.

This work has been supported by project AGRARSENSE, funded from the Chips Joint Undertaking under grant agreement No 101095835. The JU receives support from the European Union's Horizon 2020 research and innovation programme and National Funding Authorities.

References

[1] M. S. Farooq, S. Riaz, A. Abid, K. Abid and M. A. Naeem, "A Survey on the Role of IoT in Agriculture for the Implementation of Smart Farming," in IEEE Access, vol. 7, pp. 156237-156271, 2019, doi: 10.1109/ACCESS.

[2] C. Zhu, V. C. M. Leung, L. Shu and E. C. H. Ngai, "Green Internet of Things for Smart World," in IEEE Access, vol. 3, pp. 2151-2162, 2015. doi: 10.1109/ACCESS.2015.2497312

[3] T. Loh, K. Liu, F. Qin, H. Liu, "Assessment of the adaptive routing performance of a wireless sensor network using smart antennas," IET Wireless Sensor Systems, vol. 4, no. 4, pp. 195-205, 2014

[4] F. Viani, L. Lizzi, M. Donelli, D. Pregnolato, G. Oliveri, and A. Massa, "Exploitation of parasitic smart antennas in wireless sensor networks," Journal of Electromagnetic Waves and Applications, vol. 24, no. 7, pp. 993-1003, Jan. 2010.

[5] E. D. Skiani, S. A. Mitilineos, S. C. A. Thomopoulos, "A study of the performance of wireless sensor networks operating with smart antennas," IEEE Antennas and Propagation Magazine, vol. 54, no. 3, pp. 50-67, 2012.

[6] E. Taillefer, A. Hirata, and T. Ohira, "Direction-of-arrival estimation using radiation power pattern with an ESPAR antenna," IEEE Trans. Antennas Propag., vol. 53, no. 2, pp. 678–684, Feb. 2005.

[7] Groth, M.; Rzymowski, M.; Nyka, K.; Kulas, L. ESPAR Antenna-Based WSN Node With DoA Estimation Capability. IEEE Access 2020, 8, 91435–91447, doi:10.1109/ACCESS.2020.2994364.

[8] Kulas, L. RSS-Based DoA Estimation Using ESPAR Antennas and Interpolated Radiation Patterns. Antennas Wirel. Propag. Lett. 2018, 17, 25–28, doi:10.1109/LAWP.2017.2772043.

[9] Junwei Lu, D. Ireland and R. Schlub, "Dielectric embedded ESPAR (DE-ESPAR) antenna array for wireless communications," IEEE Trans. Antennas Propag., vol. 53, no. 8, pp. 2437-2443, Aug. 2005.

[10] M. Czelen, M. Rzymowski, K. Nyka and L. Kulas, "Miniaturization of ESPAR Antenna Using Low-Cost 3D Printing Process," 2020 14th European Conference on Antennas and Propagation (EuCAP), Copenhagen, Denmark, 2020, pp. 1-4.

[11] M. Czelen, M. Rzymowski, K. Nyka and L. Kulas, "Influence of Dielectric Overlay Permittivity on Size and Performance of Miniaturized ESPAR Antenna," 2020 23rd International Microwave and Radar Conference (MIKON), Warsaw, Poland, 2020, pp. 289-292.

[12] M. Czelen, M. Rzymowski, K. Nyka and L. Kulas, "Influence of Dielectric Overlay Dimensions on Performance of Miniaturized ESPAR Antenna," 2020 IEEE International Symposium on Antennas and Propagation and North American Radio Science Meeting, Montreal, QC, Canada, 2020, pp. 387-388.

[13] L. Leszkowska, M. Czelen, M. Rzymowski, K. Nyka and L. Kulas, "Miniaturized and Lightweight ESPAR Antenna for WSN and IoT Applications," 2024 18th European Conference on Antennas and Propagation (EuCAP), Glasgow, Scotland, 2024.

[14] J. Huang, S. J. Chen, Z. Xue, W. Withayachumnankul and C. Fumeaux, "Impact of Infill Pattern on 3D Printed Dielectric Resonator Antennas,"

2018 IEEE Asia-Pacific Conference on Antennas and Propagation (APCAP), Auckland, New Zealand, 2018, pp. 233-235.

[15] B. Kattel, W. E. Hutchcraft and R. K. Gordon, "Exploring Infill Patterns on Varying Infill Densities on Dielectric Properties of 3D Printed Slabs," 2023 Antenna Measurement Techniques Association Symposium (AMTA), Renton, WA, USA, 2023, pp. 1-5.